Journal of Information System and Technology Management JISTM
EISSN: 0128-1666
Volume 11 Issue 42 (March 2026) PP. 01-15

JOURNAL OF INFORMATION SYSTEM AND TECHNOLOGY MANAGEMENT (JISTM)
www.gaexcellence.com/jistm

GLOBAL ACADEMIC EXCELLENCE

AN ENHANCED DARK CHANNEL PRIOR WITH ITERATIVE TRANSMISSION UPDATE FOR SINGLE

Qin You[1]*, Mohammad Nazir Ahmad[2]

[1]Kuala Lumpur University of Science and Technology, Kajang, Selangor Darul Ehsan, Malaysia
243925342@s.klust.edu.my https://orcid.org/0009-0008-9592-6012

[2]Kuala Lumpur University of Science and Technology, Kajang, Selangor Darul Ehsan, Malaysia
Nazir@s.klust.edu.my https://orcid.org/0000-0003-3639-1157

Article Info:

Article history:
Received date: 24.12.2025
Revised date: 05.01.2026
Accepted date: 25.01.2026
Published date: 01.03.2026

To cite this document:

Qin, Y., & Ahmad, M. N. (2026). An Enhanced Dark Channel Prior with Iterative Transmission Update for Single. *Journal of Information System and Technology Management, 11* (42), 01-15.

DOI: 10.35631/JISTM.1142001

Abstract:

Hazy images suffer from visibility degradation and colour distortion due to light scattering and atmospheric attenuation, which complicates downstream vision tasks and human interpretation. The Dark Channel Prior (DCP) remains a simple yet effective physically grounded method for single image dehazing; however, it tends to underestimate transmission in bright or textureless regions (e.g., sky or specular surfaces), leading to halo artefacts and colour distortions. To address this, this paper introduces a physically interpretable corrective term from the DCP-derived transmission–radiance pair to compensate for local violations of the dark-channel assumption. The proposed method iteratively refines both the transmission map and scene radiance without requiring region segmentation. Experiments on the RESIDE and NH-HAZE datasets demonstrate that our method achieves superior PSNR, SSIM, and colour fidelity than four representative model-based dehazing algorithms, while maintaining competitive computational efficiency. Overall, the proposed iterative refinement substantially enhances the robustness and visual quality of traditional prior-based dehazing while avoiding the computational burden and data dependency of deep learning approaches.

Keyword:

Atmospheric Scattering Model, Dark Channel Prior, Iterative Transmission Update, Single Image Dehazing.

Journal of Information System and Technology Management
JISTM
EISSN: 0128-1666
Volume 11 Issue 42 (March 2026) PP. 01-15

Introduction

Atmospheric haze significantly degrades image visibility by scattering light and attenuating scene radiance, resulting in low contrast, colour distortion, and loss of detail. This degradation adversely affects downstream computer vision tasks such as surveillance, autonomous driving, and remote sensing, where reliable visual perception is crucial. Consequently, single image dehazing has become a fundamental low-level vision problem with both theoretical and practical importance.

The Dark Channel Prior (DCP), proposed by He et al. (2011), is one of the most influential physically based methods for single image dehazing. DCP assumes that in most non-sky regions of a haze-free image, at least one colour channel in a local patch has a very low intensity, enabling robust estimation of the transmission map and atmospheric light. However, the DCP tends to underestimate transmission in bright or textureless regions (e.g., sky or specular surfaces) where the near-zero assumption fails, leading to halo artefacts and colour distortion.

To address these limitations, many physically motivated extensions have been proposed. Zhu et al. (2015) introduced the Colour Attenuation Prior (CAP), which relates scene depth to brightness and saturation via a simple linear model, improving computational efficiency but suffering from non-linearity under varying illumination. Berman et al. (2020) proposed Non-local Image Dehazing based on haze-lines in RGB space, improving global transmission consistency but prone to halos near depth discontinuities. Cui et al. (2022) refined DCP in the HSI colour space (IDCP), alleviating oversaturation yet introducing colour-space dependency. Kim et al. (2024) developed a multi-DCP framework combining multiple DCP scales with adaptive air-light estimation and gamma correction, enhancing colour fidelity but increasing computational cost. Although these physically based methods achieve notable improvements, most still depend on region segmentation, multi-scale fusion, or hand-crafted heuristics, which increase algorithmic complexity and limit generalisation across diverse real-world scenes.

In parallel, deep learning-based methods such as DehazeNet (Cai et al., 2016), AOD-Net (Li et al., 2017), and GCANet (Chen et al., 2019) have achieved strong visual performance by learning end-to-end mappings from hazy to haze-free images, while transformer-based methods such as Dehamer (Guo et al., 2022) further capture global dependencies. Other notable data-driven approaches include multi-scale progressive fusion networks (Jiang et al., 2020) and methods leveraging contrastive learning (Wu et al., 2021), which aim to improve feature representation and generalizability. However, these approaches require large, paired datasets, have high computational cost, and may lack interpretability—making them unsuitable for real-time or embedded scenarios.

In this work, we focus exclusively on physically grounded methods to ensure interpretability and efficiency. We propose an Enhanced DCP with Iterative Transmission Update (E-DCP-ITU), which introduces a corrective term derived from the relationship between transmission and radiance estimated by DCP. The transmission and radiance are iteratively refined until

Journal of Information System and Technology Management
JISTM
EISSN: 0128-1666
Volume 11 Issue 42 (March 2026) PP. 01-15

convergence, followed by edge-preserving filtering (He et al., 2012). This process effectively mitigates DCP's underestimation in bright or textureless regions while maintaining low computational cost and strong physical interpretability.

The remainder of this paper is organised as follows. Section Literature Review reviews related work. Section Methodology presents the proposed methodology. Section Experiments details the experimental setup and discusses results. Section Conclusion concludes the paper.

Literature Review

Single image dehazing methods in recent years can broadly be categorised into two families: physically based approaches, which rely on the atmospheric scattering model and handcrafted priors, and learning-based approaches, which learn data-driven representations from large-scale datasets. This section briefly reviews the major developments of physically based algorithms, followed by a concise overview of data-driven trends for contextual completeness.

Physically Based Methods

Physically based dehazing algorithms are typically derived from the Atmospheric Scattering Model (ASM), originally proposed by Koschmieder, which describes the formation of a hazy image as follows:

$$I(x) = J(x)t(x) + A(1 - t(x)) \qquad (1)$$

where $I(x)$ is the observed hazy image, $J(x)$ is the scene radiance, A denotes the global atmospheric light, and $t(x)$ is the transmission map representing the portion of light that reaches the camera without scattering. The challenge lies in accurately estimating $t(x)$ and A from a single hazy image.

The DCP (He et al., 2011) provided a powerful prior for this ill-posed problem. By assuming that at least one colour channel in most non-sky patches of a haze-free image has near-zero intensity, DCP enabled effective transmission and airlight estimation. Its success inspired a large family of extensions and refinements.

CAP (Zhu et al., 2015) formulates a linear model linking scene depth to image brightness and saturation, thereby avoiding the patch-wise minimum operation required by DCP and achieving real-time performance. Non-local Image Dehazing (Berman et al., 2020) employs haze-lines in RGB space to represent the colour distribution of pixels under varying haze levels. By leveraging non-local statistics, it improves transmission smoothness and consistency, particularly in textured or sky regions. Improved DCP (IDCP) (Cui et al., 2022) operates in the HSI colour space and refines both the dark-channel computation and airlight estimation, effectively reducing over-saturation in bright areas. Most recently, Multi-DCP (Kim et al., 2024) aggregates several DCP variants computed at different scales and applies adaptive airlight estimation with gamma correction, enhancing colour fidelity and dehazing robustness. These methods collectively demonstrate that incorporating additional priors or domain-specific constraints can substantially improve the accuracy and visual quality of DCP-based results.

Despite their effectiveness, physically based methods remain constrained by hand-crafted priors and fixed parameter assumptions. Their performance may degrade in complex lighting conditions, dense haze, or scenes violating the assumed statistical distributions. Moreover,

Journal of Information System and Technology Management
JISTM
EISSN: 0128-1666
Volume 11 Issue 42 (March 2026) PP. 01-15

many extensions rely on explicit region segmentation or heuristic post-processing, which can limit generalisation.

Learning-Based Methods

Deep learning–based single image dehazing has evolved rapidly. Early supervised networks such as DehazeNet (Cai et al., 2016), AOD-Net (Li et al., 2017), and GCANet (Chen et al., 2019) used synthetic paired data to learn end-to-end mappings. Transformer-based architectures including Dehamer (Guo et al., 2022) further captured long-range dependencies. More recent research has focused on real-world generalisation and unpaired learning. For instance, Haze-Aware Attention Network (Tong et al., 2024) integrates a haze-aware attention mechanism with multi-scale frequency enhancement to recover high-frequency details. PdUNet (Jiang et al., 2024) introduces a physical-prior-guided unpaired contrastive learning framework, improving domain robustness. Learning Unpaired Image Dehazing with Physics-based Rehazy Generation (Deng et al., 2025) proposes a physics-driven "rehazy" data augmentation strategy and dual-branch network that achieves state-of-the-art performance on real hazy benchmarks. Innovative architectures like the Multi-scale Boosted Dehazing Network (Dong et al., 2020) also demonstrate the power of dense feature fusion across scales. Despite these advances, most deep models still require heavy computation or large unlabelled datasets and may hallucinate scene content, whereas our method maintains interpretability and efficiency while closing the performance gap.

Summary of Key Related Works

To systematically contextualize our research direction, we summarize the representative prior works in Table 1, highlighting their core mechanisms, strengths, and limitations.

From Table 1, we observe that while physical-based methods offer interpretability and efficiency, they often rely on handcrafted priors and fixed assumptions that fail in bright, textureless, or non-uniform haze regions (e.g., sky, specular surfaces). Most extensions introduce additional complexity through region segmentation, multi-scale fusion, or heuristic post-processing, which limits generalization and increases computational cost. On the other hand, learning-based methods achieve strong performance but at the expense of high computational demand, large data requirements, and reduced interpretability—making them less suitable for real-time or embedded applications.

Thus, a clear research gap exists: a need for a physically grounded, efficient, and robust dehazing method that does not require explicit region segmentation or complex heuristics, while maintaining interpretability and competitive performance across diverse real-world scenes.

To bridge this gap, we propose E-DCP-ITU, an enhanced dark channel prior framework that:

a. Introduces a corrective term derived from the transmission–radiance relationship to compensate for DCP's failure in bright/low-texture regions.
b. Iteratively refines transmission and radiance without requiring sky/region segmentation.
c. Preserves edge-aware smoothness via guided filtering.
d. Maintains low computational cost and strong physical interpretability, closing the performance gap with learning-based methods while avoiding their data and computation burdens.

Journal of Information System and Technology Management JISTM
EISSN: 0128-1666
Volume 11 Issue 42 (March 2026) PP. 01-15

Table 1: Summary Of Key Single Image Dehazing Methods and Their Characteristics

Method (Year)	Core Mechanism	Key Strengths	Key Limitations
DCP (2011)	Dark channel prior in local patches	Simple, physically grounded, effective for general haze	Underestimates transmission in bright/sky regions; halo artefacts; color distortion
CAP (2015)	Linear depth–brightness–saturation model	Fast, real-time suitable	Sensitive to illumination changes; limited in dense or non-uniform haze
Haze-Lines (2020)	Non-local haze-lines in RGB space	Improves transmission consistency; good for textured regions	Prone to halos near depth edges; computationally intensive
IDCP (2022)	DCP refined in HSI color space	Reduces over-saturation in bright areas	Color-space dependent; requires hand-tuned parameters
Multi-DCP (2024)	Multi-scale DCP + adaptive airlight + gamma correction	Enhanced color fidelity; robust to varying haze densities	High computational cost; complex fusion heuristics

Methodology

As outlined in Table 1, existing physical-based dehazing methods suffer from transmission underestimation in bright or textureless regions, often rely on handcrafted heuristics or region segmentation, and may introduce halo artefacts or colour distortions. Meanwhile, learning-based approaches achieve strong performance but at the cost of high computational complexity, large data dependency, and limited interpretability.

To overcome these limitations, we propose an Enhanced Dark Channel Prior with Iterative Transmission Update (E-DCP-ITU) framework. Our method introduces a corrective term derived from the DCP-based transmission–radiance pair to compensate for local violations of the dark-channel assumption, without requiring explicit region segmentation. Furthermore, we employ an iterative refinement process that jointly updates transmission and radiance, effectively mitigating DCP's underestimation in challenging regions while preserving edge details through guided filtering. This approach maintains the physical interpretability and efficiency of prior-based methods while closing the performance gap with data-driven techniques. The overall pipeline is illustrated in Figure 1.

Journal of Information System and Technology Management
JISTM
EISSN: 0128-1666
Volume 11 Issue 42 (March 2026) PP. 01-15

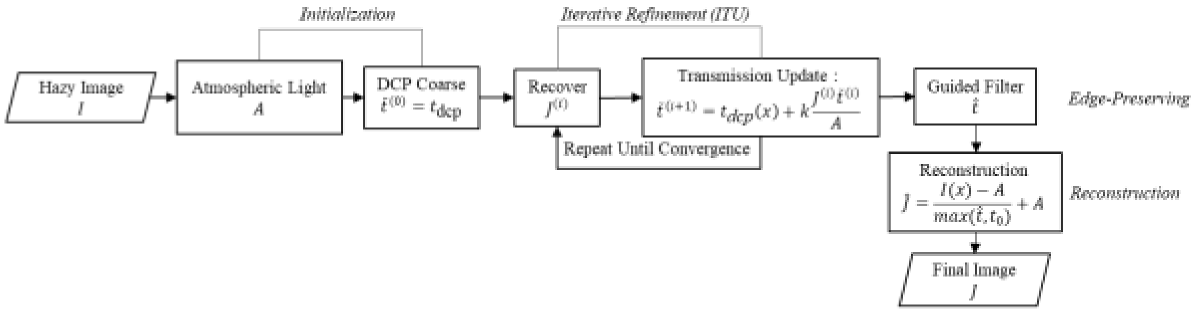

Figure 1: Overall pipeline of the proposed E-DCP-ITU

Initial Transmission Estimation

The atmospheric scattering formulation described in Eq. (1) can be rearranged as:

$$t(x) = 1 - \frac{I(x)}{A} + \frac{J(x)t(x)}{A} \quad (2)$$

The initial estimate for the transmission map is derived from the classical DCP, which assumes that in most non-sky regions of a haze-free image, at least one of the colour channels has very low intensity. This assumption leads to a reliable initial estimate for the transmission map, which can be expressed as:

$$t_{\text{dcp}}(x) = 1 - \omega \cdot \frac{I_{\text{dark}}(x)}{A} \quad (3)$$

where $I_{\text{dark}}(x)$ is the dark channel of the image, computed as:

$$I_{\text{dark}}(x) = \min_{c \in \{R,G,B\}} (\min_{y \in \Omega(x)} I^c(y)) \quad (4)$$

and ω is a constant factor (typically 0.95) controlling the strength of the DCP. The atmospheric light A is estimated from the top 0.1% brightest pixels in the image. This process gives an initial estimate of $t(x)$, which is often a good starting point but can be inaccurate in bright or textureless regions.

Corrective Term for Transmission Refinement

One limitation of DCP is that it tends to underestimate the transmission $t(x)$ in bright or low-texture regions, such as the sky or specular surfaces. This leads to halo artefacts and color distortions. To address this issue, we introduce a corrective term $f_1(x)$ derived from the initial transmission map $t_{\text{dcp}}(x)$ and the scene radiance $J(x)$. The corrective term is defined as:

$$f_1(x) = \frac{J(x)t(x)}{A} \quad (5)$$

In regions where DCP fails (such as bright or textureless areas), $J(x)$ is non-negligible, and DCP's estimate of $t(x)$ is too small. We propose an approximation for $f_1(x)$ using the initial DCP estimates:

$$f_1(x) \approx k \cdot \frac{J_{\text{dcp}}(x)t_{\text{dcp}}(x)}{A} \quad (6)$$

where k is a factor controlling the strength of the correction. This corrective term is then added to the initial transmission estimate to refine it:

Journal of Information System and Technology Management
JISTM
EISSN: 0128-1666
Volume 11 Issue 42 (March 2026) PP. 01-15

$$\tilde{t}(x) = t_{\text{dcp}}(x) + f_1(x) \tag{7}$$

Here, $J_{\text{dcp}}(x)$ is the scene radiance estimated from the initial DCP, which can be computed as:

$$J_{\text{dcp}}^{c}(x) = \frac{I^{c}(x) - A^{c}}{max\,(t_{\text{dcp}}(x), t_0)} + A^{c}, c \in \{R, G, B\} \tag{8}$$

where t_0 is a small constant (e.g., 0.05) to prevent division by zero, and A^c represents the atmospheric light for each channel.

For a more stable and efficient calculation, we can use the luminance channel $Y_{\text{dcp}}(x)$ as the intensity proxy, defined as:

$$J_{\text{dcp}}(x) = 0.299 \cdot J_{\text{dcp}}^{R}(x) + 0.587 \cdot J_{\text{dcp}}^{G}(x) + 0.114 \cdot J_{\text{dcp}}^{B}(x) \tag{9}$$

which represents the weighted sum of the RGB channels based on their perceptual contributions to the luminance.

Unlike existing variants that explicitly segment bright/sky regions to correct DCP failure, our formulation does not require spatial partitioning. This is because in regions that satisfy the dark channel prior, the latent radiance $J(x)$ is near zero, leading to $f_1(x) \approx 0$. Consequently, adding the corrective term does not change the transmission estimate, making our formulation naturally consistent with the original DCP. In regions where the prior fails, $J(x)$ becomes non-negligible so that $f_1(x)$ automatically compensates for the underestimated transmission. Hence, segmentation is unnecessary.

Iterative Transmission Update

To improve the transmission map and further reduce halo artefacts, we introduce an iterative update process. This process alternates between updating the transmission map and the scene radiance based on the atmospheric scattering model. The update procedure is as follows:

a) Initial transmission estimate:

$$\tilde{t}^{(0)}(x) = t_{\text{dcp}}(x) \tag{10}$$

b) Scene radiance update:

$$J^{(i)}(x) = \frac{I(x) - A}{max\,(\tilde{t}^{(i)}(x), t_0)} + A \tag{11}$$

c) Transmission update:

$$f_1{}^{(i)}(x) = k\frac{J^{(i)}(x)\tilde{t}^{(i)}(x)}{A} \tag{12}$$

$$\tilde{t}^{(i+1)}(x) = t_{\text{dcp}}(x) + f_1{}^{(i)}(x) \tag{13}$$

d) Convergence criteria:

$$\Delta^{(i)} = \frac{1}{N}\sum_{x \in \Omega} \mid \tilde{t}^{(i+1)}(x) - \tilde{t}^{(i)}(x) \mid \tag{14}$$

$$\Delta^{(i)} < \varepsilon \text{ or } i \geq I_{max} \tag{15}$$

where ε is a small threshold, Ω denotes the pixel domain of the transmission map, $N = \mid \Omega \mid$ is the number of pixels, and I_{max} is the maximum number of iterations. The iterative process

Journal of Information System and Technology Management
JISTM
EISSN: 0128-1666
Volume 11 Issue 42 (March 2026) PP. 01-15
terminates when the update of the transmission map falls below a predefined threshold or when the maximum number of iterations is reached.

Guided Filtering for Edge Preservation

To preserve the sharp boundaries in the image and avoid halo artefacts, we apply guided filtering to the refined transmission map. Guided filtering is an edge-preserving smoothing technique that allows us to refine the transmission map while maintaining the edges of the image. The final transmission map $\hat{t}(x)$is obtained by applying the guided filter to $\tilde{t}(x)$:

$$\hat{t}(x) = \text{guided\_filter}(\tilde{t}(x), I(x)) \qquad (16)$$

Once the transmission map has been refined, we reconstruct the final dehazed image using the refined transmission map:

$$\hat{J}(x) = \frac{I(x)-A}{max\ (\hat{t}(x), t_0)} + A \qquad (17)$$

This ensures that the dehazed image retains fine details while removing the haze.

Computational Complexity

The computational complexity of the proposed method is dominated by the iterative transmission update and the guided filtering step. Each iteration involves a per-pixel update and a local filtering step, both of which are $O(N)$, where N is the number of pixels in the image.

Experiments

Experimental Setup

Datasets

We evaluate the proposed E-DCP-ITU model on two representative paired benchmarks:
a) RESIDE(SOTS-Outdoor) A large-scale synthetic benchmark constructed using the atmospheric scattering model. It provides diverse outdoor hazy scenes enabling fair quantitative comparison.
b) NH-HAZE A real-world dataset captured under controlled conditions with corresponding haze-free references. It features non-uniform haze, strong illumination variations, and bright sky regions where many priors fail.

These two datasets complement each other: RESIDE offers controlled conditions, while NH-HAZE evaluates real-world generalization.

Baselines

We compare E-DCP-ITU against four physically based dehazing methods:
a) DCP (He et al.),
b) CAP (Zhu et al.),
c) Haze-Lines (Berman et al.),
d) Multi-DCP (Liu et al.).

Journal of Information System and Technology Management
JISTM
EISSN: 0128-1666
Volume 11 Issue 42 (March 2026) PP. 01-15

All baselines are implemented following their original papers with identical recovery models for fair comparison.

Evaluation Metrics

Metrics are computed on normalized RGB $[0,1]$against aligned ground-truth images. We adopt three widely used metrics for paired image dehazing evaluation:

a) Peak Signal-to-Noise Ratio (PSNR, ↑ better),
b) Structural Similarity (SSIM, ↑ better),
c) perceptual color difference ΔE (CIEDE2000, ↓ better).

All quantitative results are reported as the arithmetic mean of PSNR, SSIM, and ΔE over the entire test set. For consistency, PSNR is rounded to two decimal places, SSIM to four decimal places, and ΔE to two decimal places.

Implementation Details

We adopt the same atmospheric scattering formulation described in Section Physically based methods. For the classical DCP, we use $\omega = 0.95$, patch radius $r = 7$, and transmission lower bound $t_0 = 0.05$. Our iterative formulation follows Eq. (11) in Section 3. Guided filtering is used for edge-preserving refinement (radius=32, $\varepsilon = 10^{-3}$).

Hyperparameter Selection

To determine the optimal iterative weight k and maximum update count $I_{\max}$, we perform a grid search using NH-HAZE: $k \in \{0.0, 0.1, \dots, 0.9, 1.0\}$, $I_{\max} \in \{1,2,3,4\}$. For each candidate configuration, we compute the averaged PSNR, SSIM, and ΔE over all the images of NH-HAZE.

In typical outdoor scenes, the three metrics (PSNR↑/SSIM↑/ΔE↓) are measured on heterogeneous numerical scales, direct averaging would lead to biased comparisons. PSNR varies perceptibly by ≈1–3 dB, SSIM is sensitive to ≈ 0.01, ΔE changes of ≈ 1 is usually visually noticeable. So, we adopt a perceptual-unit normalization; the composite score is defined as:

$$\text{Score} = \frac{PSNR}{1} + \frac{SSIM}{0.01} - \frac{\Delta E}{1} \qquad (18)$$

This strategy balances structure preservation, signal fidelity, and color consistency on comparable scales. The best configuration was found to be: $k = 0.8$, $I_{\max} = 2$.

Runtime Protocol

We report per-image execution time (in milliseconds) for all baselines (DCP, CAP, Haze-Lines, Multi-DCP) and our E-DCP-ITU. Following common practice, timing excludes I/O and visualization and covers only the dehazing function call. Each method is executed once per test image; we then report the mean, median, standard deviation, minimum, and maximum across the test set.

Journal of Information System and Technology Management JISTM
EISSN: 0128-1666
Volume 11 Issue 42 (March 2026) PP. 01-15

All experiments were executed on a machine equipped with an AMD Ryzen 7 7840HS processor with integrated Radeon 780M graphics and 32 GB RAM running Windows 11. The implementation was based on Python 3.10 with NumPy 1.26.4 and scikit-image 0.22.0.

Results on RESIDE (SOTS-Outdoor)

As can be seen from Table 2, our method achieves the highest PSNR and SSIM, outperforming DCP by 2.77 dB PSNR and Multi-DCP by 4.46 dB PSNR. E-DCP-ITU yields the lowest ΔE, indicating improved color fidelity.

Table 2: Quantitative Comparison On SOTS-Outdoor

Method	PSNR	SSIM	ΔE
DCP	16.22	0.7923	15.27
CAP	12.43	0.3890	26.61
Haze-Lines	12.90	0.3137	19.79
Multi-DCP	14.53	0.4666	17.82
E-DCP-ITU(Ours)	**18.99**	**0.8194**	**10.94**

Note: Best in Bold.

Figure 2 presents visual examples from the RESIDE (SOTS-Outdoor) dataset, including the hazy input, results from four representative reference methods, our E-DCP-ITU approach, and the ground-truth image. DCP produces over-dehazed regions with darkening artifacts. CAP reduces color distortion but frequently yields dim images. Haze-Lines removes haze unevenly, leaving some areas hazy while making others too dark. Multi-DCP remains unstable restoring color in some regions while making others too dark. In contrast, our E-DCP-ITU preserves natural brightness and color, producing clearer structures and more balanced haze removal.

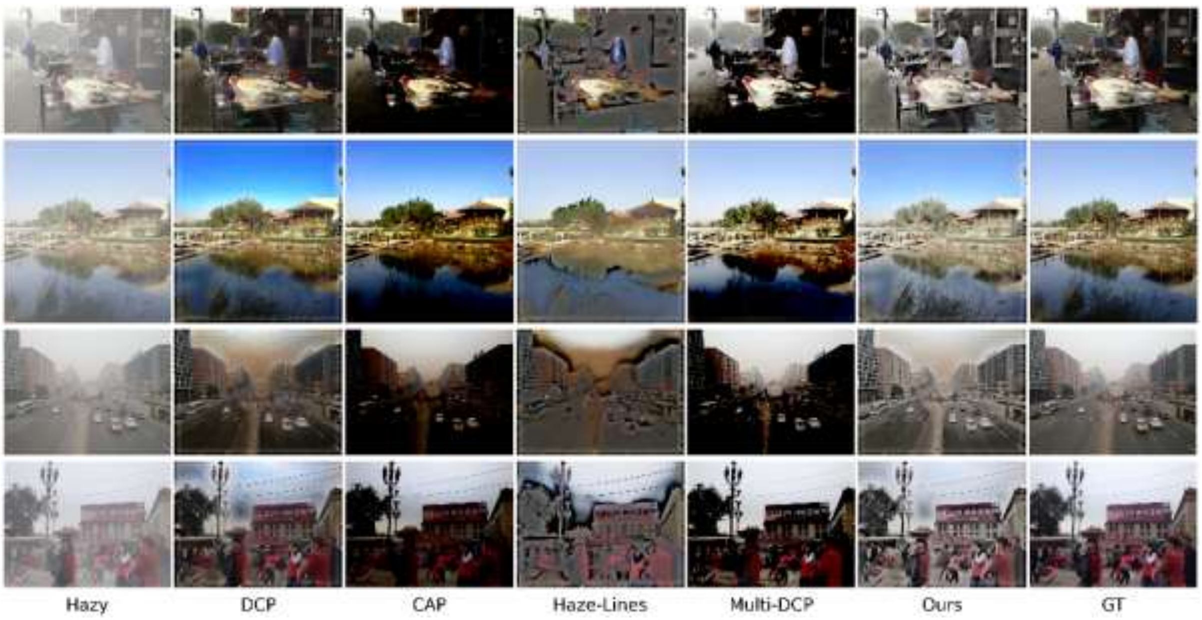

Figure 2: Qualitative Comparison on RESIDE (SOTS-Outdoor)

Journal of Information System and Technology Management
JISTM
EISSN: 0128-1666
Volume 11 Issue 42 (March 2026) PP. 01-15

Results on NH-HAZE

Our method maintains stable gains in real haze. As can be seen from Table 3, PSNR increases by 1.01 dB compared to DCP and 3.21 dB over multi-DCP; ΔE also greatly decreases, demonstrating faithful color recovery under challenging illumination.

Figure 3 shows NH-HAZE visual results. The overall trends are consistent with those on RESIDE (SOTS-Outdoor), but performance declines across all methods due to NH-HAZE's more non-uniform and complex haze distribution. DCP still produces over-dehazed and darkened regions, similar to its behavior on RESIDE. CAP, Haze-Lines, and Multi-DCP generally struggle with insufficient haze removal, especially in distant or low-texture regions, leaving noticeable residual haze. In contrast, our E-DCP-ITU provides the most visually balanced restoration with clearer structures and more natural colors, though the improvement margin is smaller compared with RESIDE.

Table 3: Quantitative Comparison On NH-HAZE

Method	PSNR	SSIM	ΔE
DCP	12.16	0.4672	32.27
CAP	10.38	0.2908	36.70
Haze-Lines	9.97	0.1771	36.50
Multi-DCP	9.96	0.2964	35.67
E-DCP-ITU(Ours)	**13.17**	**0.5354**	**25.98**

Note: Best in Bold.

Figure 3: Qualitative Comparison On NH-HAZE

These observations align with the quantitative results, where PSNR and SSIM values are overall lower and ΔE values are higher on NH-HAZE, reflecting the increased difficulty of removing spatially varying haze.

Runtime

Table 4: Runtime Statistics On NH-HAZE

Method	mean	median	std	min	max
CAP	357.36	323.00	75.56	307.37	596.62
DCP	823.58	741.17	183.34	731.81	1596.09
E-DCP-ITU(Ours)	945.20	857.40	195.63	848.74	1684.26

Haze-Lines	2721.78	2469.69	471.62	2403.23	4166.27
Multi-DCP	7110.66	6374.89	1527.06	6320.86	12779.37

We further evaluate processing time on NH-HAZE. Table 4 reports the runtime statistics of the five evaluated representative dehazing algorithms. CAP is the fastest method, with an average per-image runtime of 357.36 ms, owing to its lightweight prior and simple formulation. DCP is slightly slower (mean 823.58 ms) but remains computationally efficient. Our E-DCP-ITU achieves a mean runtime of 945.20 ms, which is moderately slower than DCP due to the iterative refinement but still substantially faster than Haze-Lines (2721.78 ms) and multi-DCP (7110.66 ms). Notably, ITU shows low variance (std = 195.63 ms), indicating stable behavior. Haze-Lines is roughly 3× slower than ours, whereas multi-DCP is as much as 7.5× slower, mainly because of additional multi-branch prior computation. These results confirm that our proposed refinement remains computationally light, achieving a favorable balance between efficiency and restoration quality.

Discussion

Experiments on RESIDE and NH-HAZE show that E-DCP-ITU achieves the best balance among visual quality, quantitative accuracy, and computational efficiency. It mitigates DCP over-dehazing, preserves colors more faithfully than CAP, and avoids instability in Haze-Lines and Multi-DCP. Although performance decreases on NH-HAZE due to its irregular haze, our method remains superior. Runtime is only modestly higher than DCP and notably faster than Haze-Lines and Multi-DCP, confirming the practicality of E-DCP-ITU.

Overall, the results confirm that E-DCP-ITU offers a compelling trade-off among accuracy, robustness, and efficiency, making it suitable for practical deployment. Future work includes incorporating spatially adaptive iteration control and learned priors to further enhance robustness in complex haze environments.

Conclusion

This paper presented E-DCP-ITU, an enhanced dark-channel-prior–based single-image dehazing framework that introduces an iterative transmission update (ITU) to address the transmission underestimation issue inherent in classical DCP, particularly in bright and low-texture regions. By leveraging a corrective term derived from the course DCP radiance–transmission pair, the proposed method progressively refines the transmission map without requiring explicit sky/region segmentation. A guided filtering stage further preserves structure and prevents halo artifacts during radiance reconstruction.

Extensive experiments on RESIDE (SOTS-Outdoor) and NH-HAZE demonstrate that E-DCP-ITU consistently delivers improved visual fidelity and higher quantitative accuracy (PSNR, SSIM, ΔE), outperforming all baselines (DCP, CAP, Haze-Lines, Multi-DCP). The method effectively suppresses over-dehazing and color distortion while producing better structural clarity. Although all methods degrade on NH-HAZE due to its spatially complex haze distribution, E-DCP-ITU maintains the most balanced results. Runtime evaluations reveal that E-DCP-ITU introduces only moderate computational overhead compared to DCP while remaining significantly faster than Haze-Lines and Multi-DCP, offering a favorable efficiency–performance trade-off.

Overall, E-DCP-ITU demonstrates that the integration of model-based priors with iterative radiance–transmission correction yields robust and effective haze removal, without reliance on heavy learning or external training data. Future work will explore adaptive iteration scheduling, scene-aware refinement, and hybrid learning–physics components to further enhance performance in highly heterogeneous and nighttime haze scenarios.

Acknowledgements:	The authors would like to express their sincere gratitude to Kuala Lumpur University of Science and Technology for providing the necessary resources and support throughout the course of this research. Special appreciation is extended to colleagues and peers who contributed valuable insights and constructive feedback, which greatly enhanced the quality of this paper.
Funding Statement:	No Funding
Conflict of Interest Statement:	The authors declare that there is no conflict of interest regarding the publication of this paper. All authors have contributed to this work and approved the final version of the manuscript for submission to the Journal of Information System and Technology Management (JISTM)
Ethics Statement:	This study did not involve any human participants, animals, or sensitive data requiring ethical approval. The authors confirm that the research was conducted in accordance with accepted academic integrity and ethical publishing standards.
Author Contribution Statement:	All authors contributed significantly to the development of this manuscript. Qin You was responsible for the conceptualization, methodology, and overall supervision of the study. Qin You handled data collection, analysis, and interpretation of results. Mohammad Nazir Ahmad contributed to the literature review, drafting, and critical revision of the manuscript. All authors read and approved the final version of the manuscript prior to submission.

Journal of Information System and Technology Management
JISTM
EISSN: 0128-1666
Volume 11 Issue 42 (March 2026) PP. 01-15

References

Berman, D., Treibitz, T., & Avidan, S. (2020). Single image dehazing using haze-lines. *IEEE Transactions on Pattern Analysis and Machine Intelligence, 42*(3), 720–734. https://doi.org/10.1109/TPAMI.2018.2882478

Cai, B., Xu, X., Jia, K., Qing, C., & Tao, D. (2016). DehazeNet: An end-to-end system for single image haze removal. *IEEE Transactions on Image Processing, 25*(11), 5187–5198. https://doi.org/10.1109/TIP.2016.2598681

Chen, D., He, M., Fan, Q., Liao, J., Zhang, L., Hou, D., Yuan, L., & Hua, G. (2019). Gated context aggregation network for image dehazing and deraining. In *Proceedings of the IEEE Winter Conference on Applications of Computer Vision (WACV)* (pp. 1375-1383). https://doi.org/10.1109/WACV.2019.00151

Cui, Y., Zhi, S., Liu, W., Deng, J., & Ren, J. (2022). An improved dark channel defogging algorithm based on the HSI colour space. *IET Image Processing, 16*(3), 823–838. https://doi.org/10.1049/ipr2.12389

Dong, H., Pan, J., Xiang, L., Hu, Z., Zhang, X., Wang, F., & Yang, M. H. (2020). Multi-scale boosted dehazing network with dense feature fusion. In *Proceedings of the IEEE/CVF Conference on Computer Vision and Pattern Recognition (CVPR)* (pp. 2157-2167). https://doi.org/10.1109/CVPR42600.2020.00223

Deng, H., Li, Z., Zhang, F., Lu, Q., Cao, Z., Shao, Y., Gu, S., Gao, C., & Sang, N. (2025). Learning unpaired image dehazing with physics-based rehazy generation. *arXiv*. https://doi.org/10.48550/arXiv.2506.12824

Guo, C. L., Yan, Q., Anwar, S., Cong, R., Ren, W., & Li, C. (2022). Image dehazing transformer with transmission-aware 3D position embedding. In *Proceedings of the IEEE/CVF Conference on Computer Vision and Pattern Recognition* (pp. 5812-5820). https://openaccess.thecvf.com/content/CVPR2022/html/Guo_Image_Dehazing_Transformer_With_Transmission-Aware_3D_Position_Embedding_CVPR_2022_paper.html

He, K., Sun, J., & Tang, X. (2011). Single image haze removal using dark channel prior. *IEEE Transactions on Pattern Analysis and Machine Intelligence, 33*(12), 2341–2353. https://doi.org/10.1109/TPAMI.2010.168

He, K., Sun, J., & Tang, X. (2012). Guided image filtering. *IEEE Transactions on Pattern Analysis and Machine Intelligence, 35*(6), 1397–1409. https://doi.org/10.1109/TPAMI.2012.213

Jiang, A., Wu, M., Liu, F., Liu, B., & Zhang, C. (2024). PDUNet: Physical-prior-guided single image dehazing network via unpaired contrastive learning. *SSRN*. https://doi.org/10.2139/ssrn.4682033

Jiang, K., Wang, Z., Yi, P., Chen, C., Huang, B., Luo, Y., ... & Jiang, J. (2020). Multi-scale progressive fusion network for single image deraining. In *Proceedings of the IEEE/CVF conference on computer vision and pattern recognition* (pp. 8346-8355). https://openaccess.thecvf.com/content_CVPR_2020/html/Jiang_Multi-Scale_Progressive_Fusion_Network_for_Single_Image_Deraining_CVPR_2020_paper.html

Kim, J., Ng, T. S., & Teoh, A. B. J. (2024). Enhancing image dehazing with a multi-DCP approach with adaptive airlight and gamma correction. *Applied Sciences, 14*(17), 7978. https://doi.org/10.3390/app14177978

Li, B., Peng, X., Wang, Z., Xu, J., & Feng, D. (2017). AOD-Net: All-in-one dehazing network. In *Proceedings of the IEEE International Conference on Computer Vision (ICCV)* (pp. 4770-4778). https://doi.org/10.1109/ICCV.2017.511

Tong, L., Liu, Y., Li, W., Chen, L., & Chen, E. (2024). Haze-aware attention network for single-image dehazing. *Applied Sciences, 14*(13), 5391. https://doi.org/10.3390/app14135391

Wu, H., Qu, Y., Lin, S., Zhou, J., Qiao, R., Zhang, Z., ... & Ma, L. (2021). Contrastive learning for compact single image dehazing. In *Proceedings of the IEEE/CVF Conference on Computer Vision and Pattern Recognition (CVPR)* (pp. 10551-10560). https://openaccess.thecvf.com/content/CVPR2021/html/Wu_Contrastive_Learning_for_Compact_Single_Image_Dehazing_CVPR_2021_paper.html

Zhu, Q., Mai, J., & Shao, L. (2015). A fast single image haze removal algorithm using color attenuation prior. *IEEE Transactions on Image Processing, 24*(11), 3522–3533. https://doi.org/10.1109/TIP.2015.2446191